Applied Thermal Engineering 205 (2022) 118011

Contents lists available at ScienceDirect

Applied Thermal Engineering

journal homepage: www.elsevier.com/locate/apthermeng

Design and experimental evaluation of phase change material based cooling ceiling system

Jan Skovajsa *, Pavel Drabek, Stanislav Sehnalek, Martin Zalesak

Faculty of Applied Informatics, Tomas Bata University in Zlin, CEBIA-Tech, Nad Stranemi 4511, 760 05 Zlin, Czech Republic

ARTICLE INFO

Keywords:
Cooling ceiling
Energy savings
Heat accumulation
PCM
TES
2010 MSC:
00-01
99-00

ABSTRACT

This article deals with the possibility of using PCMs in cooling ceiling systems to reduce significantly air temperature fluctuations and energy demands for cooling. The PCM-based cooling ceiling's technical design was performed, and a prototype was realized in this research. The experimental verification of the proposed system was performed to determine the actual parameters in different operational modes and their comparison with the same cooling ceiling system without PCM. The transient simulations in the TRNSYS simulation software were also carried out and validated with experiments. Based on the findings, the complex simulations were performed for application under the specific climatic conditions of Czechia. This work contains a comprehensive approach from the prototype design, through the experiments and partial simulations, to complex simulations based on the specific parameters and an economic evaluation. The results of this work show the ability of the proposed cooling ceiling solution to reduce temperature peaks by up to 3.2 °C, while energy savings can be up to 27%, depending on the air change rate. These results can also help significantly determine the economic feasibility of a PCM-based solution for ceiling cooling systems.

1. Introduction

The building and construction sector is one of the most crucial sectors concerning energy consumption in the world. In 2018, this sector represented up to 36% of final energy consumption and 39% of energy-related carbon dioxide (CO2) emissions related to energy and building processes [1].

Reducing the energy consumption of buildings is the subject of the Directive 2010/31/EU of the European Parliament and the Council on the energy performance of buildings (EPDB) [2], as amended by Directive 2018/844/EU of the European Parliament and the Council [3]. The emphasis is on increasing the energy efficiency of technological systems, reducing CO2 emissions, and increasing the share of alternative (renewable) energy sources.

Over the last two decades, great emphasis has been placed on improving the thermal insulation of the building envelope. Practice shows that these ways of reducing the energy performance of buildings are currently close to their limits, and additional energy savings are achieved only by a disproportionate increase of investments. Other parts of buildings that contribute to the overall energy consumption and still show some reserves are building automation and the technology systems themselves. Therefore, the intentions above call for studies dealing with the issues of individual parts of heating, ventilation, and air conditioning (HVAC) systems and modern materials.

All efforts have one primary aim - to reduce global final energy consumption and energy-related CO2 emissions. However, there are also problems associated with these trends that need to be addressed. Modern buildings increasingly consist of standardized components made of lightweight materials such as thin metals, lightweight concrete, wood, plastic, and plasterboard [4]. These constructions mostly have high-quality insulation standards, which corresponds to worldwide requirements. On the other hand, they may have an insufficient heat storage capacity. These facts can lead to problems with temperature fluctuations and overheating in summer. Heat accumulation is addressed in direct relation from the point of view of assessing current technical solutions and scientific approaches. More precisely, it is about the possibility of applying thermal energy storage (TES) and phase change materials (PCM). Accumulation of heat has been receiving more attention in the last few years because it is a possible way to address the building sector's thermal stability and energy consumption issues.

The article includes an introductory part concerning the thermal stability of buildings and the possibilities of its improvement by TES. It also contains parts describing the experiments, and simulations and an

* Corresponding author.
E-mail address: jskovajsa@utb.cz (J. Skovajsa).

https://doi.org/10.1016/j.applthermaleng.2021.118011
Received 24 August 2021; Received in revised form 16 November 2021; Accepted 27 December 2021
Available online 3 January 2022

Nomenclature

A_a	Active cooling area (m^2)
P	Total cooling capacity (W)
P_a	Specific cooling capacity (Wm^{-2})
$\dot{m}$	Mass flow rate ($kg{\cdot}s^{-1}$)
c_p	Specific heat capacity ($Jkg^{-1}K^{-1}$)
T	Temperature (K)
ΔT	Temperature Difference (K)
θ_{air}	Air temperature (°C)
θ_{globe}	Globe temperature (°C)
θ_{comp}	Air temperature in compensation (°C)
$\theta_{w,out}$	Outlet water temperature (°C)
$\theta_{w,in}$	Inlet water temperature (°C)
ACH	Air Change Rate ($1{\cdot}h^{-1}$)
RMSE	Root Mean Square Error (–)
RRMSE	Relative Root Mean Square Error (–)
R2	Coefficient of determination (–)
NPV	Net Present Value (€)
IRR	Internal Rate of Return (%)
DPP	Discounted Payback Period (year)
VAT	Value Added Tax (%)
CCC	Compensated Calorimetric Chamber
CEBIA-Tech	Centre for Security, Information and Advanced Technologies
CO2	Carbon Dioxide
COP	Coefficient of Performance
DSC	Differential Scanning Calorimetry
EER	Energy Efficiency Ratio
FAI	Faculty of Applied Informatics
HP	Heat Pump
HRV	Heat Recovery Ventilation
HVAC	Heating, Ventilation, and Air Conditioning
IR	Infrared
LEE	Laboratory of Environmental Engineering
PCM	Phase Change Materials
PVC	Polyvinyl Chloride
RES	Renewable Energy Sources
TBU	Tomas Bata University
TES	Thermal Energy Storage
TRNSYS	Transient Systems Simulation Software

evaluation of the obtained results, including the economic assessment.

2. Current state of knowledge

2.1. Thermal stability of building

With the increasing application of lightweight materials in building structures, the set requirements for thermal insulation are being met. However, due to the low thermal storage capacity of these materials, thermal stability problems can occur. This is crucial for installing and determining mechanical cooling parameters, significantly increasing the building's energy intensity [5].

The architectural and construction solution of buildings should ensure low energy consumption while meeting suitable conditions of the indoor microclimate. Furthermore, the construction and operational solution should be such that the demand for cooling is minimized or mechanical cooling is unnecessary [6]. Various solutions can reduce energy intensity, such as suitable size and orientation of glazed surfaces, shading, thermal-storage materials, suitable ventilation regime, and use of renewable energy sources (RES) [6].

For lightweight buildings, the thermal storage capacity is usually reduced, but the installation of heavy structures can partially compensate for it (e.g., ceilings and internal walls). Another way to improve thermal storage capacity is to apply TES and thermal storage elements such as PCMs.

2.2. Thermal energy storage

TES's basic principles are based on temperature changes (sensible TES), phase changes (latent TES), or thermochemical processes.

The accumulation of sensible heat is an important parameter of materials in building construction. Each material can accumulate a certain amount of heat and emit it back to the ambient. The specific heat capacity gives this ability. Lightweight structures have a low heat capacity and are predisposed to temperature fluctuations [7]. The latent heat storage systems are based on absorbing or releasing heat during the phase change processes from solid to liquid, liquid to gas, or vice versa. This method is helpful due to the high density of stored energy per unit weight [8].

TES is a possible way to successfully reduce the negative effects of sufficient thermal stability and increase energy use efficiency in the building. It represents the possibility of temporary thermal energy storage, in the form of heat or cold, for later utilization [9]. It can partially cover part of the energy deficit, usually covered by external sources.

2.3. Phase change materials

Phase change materials are used to store thermal energy. These are very useful for their ability to absorb large amounts of latent energy during a phase change. The liquid to solid phase change, i.e., melting and solidification, is most used [10].

The choice of suitable PCMs depends on the specific practical application and properties, such as physical, chemical, and thermal parameters [10]. The basic selection is based on the phase change temperature range for the specific application. The range between 10 °C and 60 °C is suitable for applications in HVAC and building constructions [12].

PCMs suitable for building applications can be further divided into temperature categories according to how they are used [13,12]: The phase change temperature range of 10 °C to 22 °C is recommended for cooling; The temperature range between 22 °C and 28 °C is suitable for applying PCM into building structures as passive elements to ensure optimal thermal comfort; PCMs with a phase change temperature range from 29 °C to 60 °C are used for applications using hot water, e.g., floor heating with accumulation.

2.4. PCMs applications

Practical PCM applications represent a wide range of possible solutions, both as part of building structures and TES systems. They can be categorized as passive and active building systems. Heier et al. [14] state that passive storage is charging and discharging by temperature difference between the storage and the surroundings. In the case of active storage, the active pumps or fans are utilized. There are also combinations where the charging is active, and the discharging is passive or vice versa.

Passive building systems use the incorporation of PCMs into building components such as floors [15], walls [16–20], roofs and ceilings [21–27], transparent elements [28–30], and shading solution [31]. The integration of PCM changes the thermal-storage properties of the building structures. In general, PCM integration can improve a natural

regulation of thermal comfort by reducing heat transfer rates and temperature fluctuations [32,33], there is also a time shift, and distribution of the peak heat load [21,34]. Moreover, the effective incorporation of PCM can reduce the operational time of HVAC systems [35], which can lead to energy savings. The passive cooling systems suit high diurnal temperature differences, so the PCM is mainly cooled by night-time natural cooling. During cooling, the PCM solidifies, and when the ambient temperature rises, the accumulated cold is released. Thus, PCM can cover part of the cooling load during the daytime.

As was mentioned, active pumps or fans are utilized in active cooling systems. So, these systems are commonly based on the integration of PCMs with mechanical ventilation [36–40] or water system [41,24,25,42–46]. It is possible to achieve optimal thermal comfort and better energy utilization leading to energy savings by a suitable combination of PCM and HVAC.

Many published research focused on the impact of PCM integration into cooling systems on the dynamic behavior of building and its technology systems, which is supported by outputs from various simulation tools or experiments.

Rucevskis et al. [23] presented a simulation-based study of the PCM-based TES for space cooling. Results showed that installation of the active TES system has a positive effect on thermal comfort for the specific Baltic climate. The results also showed reducing the average indoor air temperature by up to 6.8 °C, but the authors stated the most extreme scenario was considered in this study. Nielsen et al. [47] numerically investigated PCM-based cooling ceiling with night cooling strategy and observed 15% and 17% peak load reductions for Copenhagen and Rome. Allerhand et al. [34] presented numerical energy performance evaluation of PCM ceiling panels. Their results show the PCM panels could save energy by 14%. Gallardo and Berardi [48] numerically evaluated the energy and thermal performance of a radiant cooling panel system with PCMs for application in building retrofit projects. The results show that the radiant system is able to provide adequate indoor thermal comfort conditions and yield energy savings of around 48% compared to the all-air system in very hot and humid climate conditions. The authors assumed the air change rate for the PCM system is considerably lower than that of the all-air system. Stefansen et al. [49] numerically examined the performance of PCM in active ceiling panels under different climates conditions. The study showed that the PCM model provided a more comfortable thermal indoor environment, disregarding the climate. However, the results showed a significant impact of climatic conditions on energy savings. The most considerable energy savings, over 30%, was found for cold climates. Results for other climates showed energy savings from −20% to 24%.

Pavlov [21] experimentally investigated PCM-clayboard ceiling panels. Around 32% of peak power reduction and reducing the daytime peak temperatures by up to 3 K was achieved in this study. Weinläder et al. [24,25] assessed the dynamical thermal behavior (passive cooling and regeneration behavior) of two PCM cooling ceilings prototypes in the Energy Efficiency Center. The proposed prototypes reached adequate thermal performance. Bourdakis et al. [41] experimentally examined active PCM radiant cooling ceiling panels. The results showed the active discharging is more effective than passive. Bogatu et al. experimentally tested the performance of the ceiling panels with and without PCM. In the first research, they revealed problems with the inadequate capacity of heat storage, inappropriate panel construction, and low thermal conductivity [26]. Their recent study with macro-encapsulated PCM ceiling panels shows that the active ceiling maintained an indoor thermal environment close to what was achieved by the conventional cooling panels [27].

Most available studies show that PCM-based cooling ceilings can achieve optimal thermal comfort and better energy utilization than conventional cooling systems. However, the results also showed a significant impact of climatic conditions on energy savings.

Moreover, most of the previous articles are focused on numerical or experimental research separately. Numerical simulations are very valuable but may contain several assumptions, for example, input data from manufacturer's catalogs or spreadsheets, that may cause inaccuracies of the results; therefore, they may not be sufficient to obtain accurate results without experimental validation. So, the cooling ceiling systems with PCM integration need to be further experimentally investigated under different conditions with regard to temperature and energy performance. In the literature, it was found that very few researchers have focused on the economic aspects of using PCM in cooling ceiling systems.

The present study is concerned with the feasibility of integrating PCM into the prototype of a cooling ceiling system. A prototype has been suggested that is not only numerical simulated but also experimentally validated. The experiments were performed to determine the actual parameters in different operational modes and their comparison with a same cooling ceiling system without PCM. The present study analyzed the impact of PCM integration on cooling performance, thermal comfort, and cooling energy savings for the specific climate of Czechia (Temperate, Central Europe). In the study, there was also performed financial performance analysis.

Table 1
Thermal and physical parameters of PCM Energain [50,51].

Parameter	Value	Unit
Area density	4.5	$kg \cdot m^{-2}$
Density	855	$kg \cdot m^{-3}$
Melting point (peak value)	21.7	°C
Latent heat of melting and solidification	>70	$kJ \cdot kg^{-1}$
Total heat capacity (0 °C to 30 °C)	>170	$kJ \cdot kg^{-1}$
Thermal conductivity (liquid)	0.18	$W \cdot m^{-1}K^{-1}$
Thermal conductivity (solid)	0.22	$W \cdot m^{-1}K^{-1}$
Flash point (paraffin)	148	°C

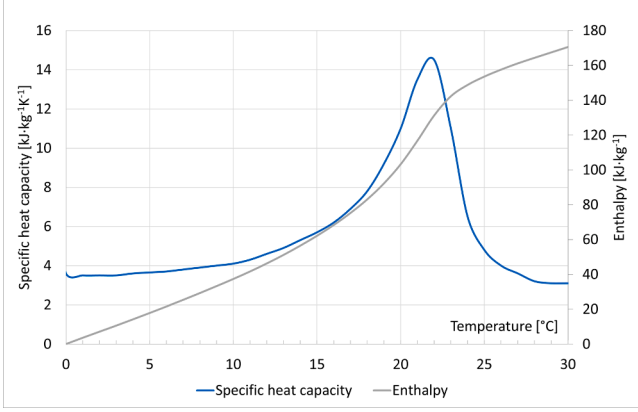

Fig. 1. DSC curve for PCM Energain.

3. Methodology

This research paper consists of several interrelated parts leading to the determination of the effect of the use of PCM in cooling ceilings. This section describes the specific PCM material used in the presented research, the laboratory facilities used, the measuring equipment, the design of the prototype of the innovative cooling ceiling, the measurement methods and the setup of the simulation models.

3.1. PCM DuPont Energain

The paraffin-based PCM Energain from DuPont was used in the experiments. This material is in the form of panels with dimensions 1000 × 1198 × 5.26 mm. The panels are laminated on both sides with a layer

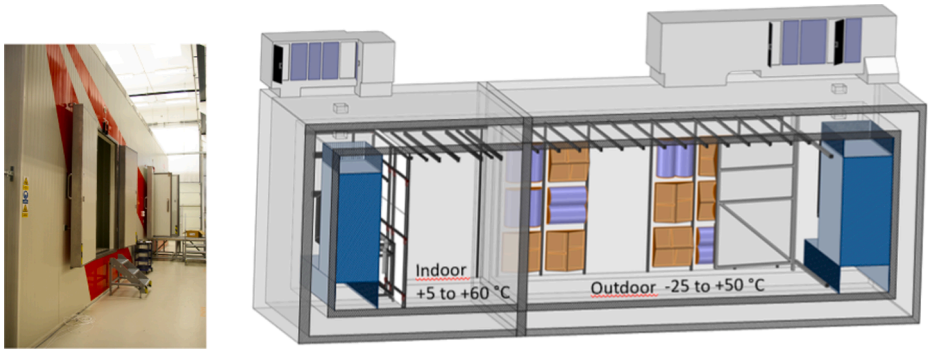

Fig. 2. Outer shell and 3D model of the chamber.

of aluminium with a thickness of 130 μm. The core material is a mixture of 60% of molecular encapsulated paraffin wax and 40% of polymer. The PCM Energain uses molecular encapsulation developed by DuPont, which allows a very high concentration of PCM within a polymer compound. Molecular encapsulation forms a highly durable PCM material with a wide operating temperature range and allows drilling and cutting through the material without the risk of PCM leakage. The PCM parameters are shown in the following Table 1 [50].

Fig. 1 shows a Differential Scanning Calorimetry (DSC) curve for PCM Energain (0.5 K·min^{-1}).

The melting and solidification temperature range of the selected material is between 18 °C and 24 °C. This is suitable for passive systems applications, ensuring thermal comfort and an active system, e.g., space cooling. The core of the PCM has a flashpoint of 148 °C, which can be considered safe for low and medium temperature applications under consideration, i.e., from 10 °C to 40 °C.

Fig. 4. The PCM-based cooling ceiling box prototype.

3.2. The laboratory facilities and measuring equipment

The research was carried out in the Laboratory of Environmental Engineering (LEE), part of the regional research center CEBIA-Tech at Tomas Bata University, Faculty of Applied Informatics (FAI TBU) in Zlin. [52]. The major part of the LEE is the universal compensated calorimetric chamber (CCC), see Fig. 2. The CCC is designed as a double-layer construction with a temperature-adjustable interspace to compensate for the influence of the external laboratory environment. The interior space is further divided by a calibrated, demountable partition that splits the internal (reconditioning) space into two separate compartments.

Different microclimatic conditions can be ensured in the reconditioning spaces. Required values can be set for different tests according to the relevant standards. For preparing hot and cold liquid for external applications, the Indoor reconditioning space is also equipped with a precisely controllable and measured mobile heat exchanger station connected to the cold and hot circuit of the reconditioning unit.

It is possible to measure parameters of various devices and HVAC components in CCC, such as air conditioning, air-to-air and air-to-water heat pumps, cooling ceilings and beams, fan heaters, selected ventilation distribution elements, and measurement of acoustic parameters of various devices and materials. Thanks to the possibilities and capacities, the CCC was also be used for experiments within the presented research.

Following measuring equipment was used during the experiments:

- Relative humidity (RH) and temperature - Rotronic HF532-WBA3D1XX (±0.8%RH, ±0.1 K)
- Electromagnetic flow sensor - KROHNE OPTIFLUX2000 (±0.5%)
- Temperature probe Pt100 - Greisinger GTF101P (1/10 DIN class B)
- Thermocouples - Almemo ZA9020-FS with NiCr-Ni thermowire T 190-1 (±0.1 K, calibrated by the thermal bath Lauda ECO RE 1050 S)
- Globe thermometer - Almemo FPA805GTS (Pt100 DIN class B)
- Heat Flow Plates - Almemo FQA018C (±5%)
- Power and energy metering module - B&R X20AP3131 (±1.8%)
- IR camera - Fluke Ti45 Thermal Imager

3.3. PCM-based cooling ceiling system - design

The technical solution dealt with the design of individual parts of the system: composition of the cooling ceiling box with PCM, installation in CCC, and the system's hydraulic circuit. It should be connected to the cooling and heating circuit of the Indoor reconditioning unit in CCC, preferably as a secondary circuit.

The schema in Fig. 3 shows a section of the cooling ceiling box. The shell of this box is made of 1.5 mm thick sheet metal with a matte white finish. Dimensions of the shell are 1.6 × 0.8 × 0.2 m. The box is filled with a layer of PCM Energain and equipped with a tube heat exchanger in direct contact with the PCM.

Fig. 4 shows a prototype of the PCM-based cooling ceiling box.

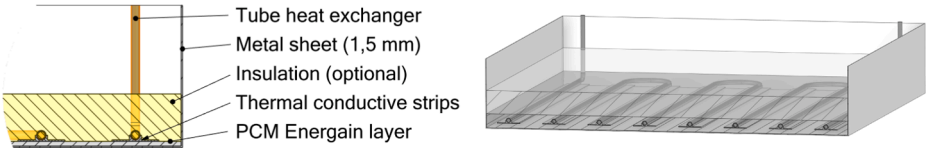

Fig. 3. Composition of the ceiling cooling box with PCM.

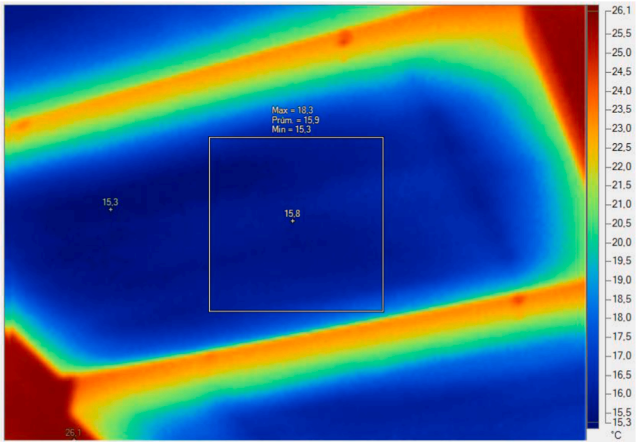

Fig. 5. IR image of cooling ceilings with PCM.

The distribution of surface temperature is important, especially for elements with PCMs. For this purpose, the tube heat exchanger is equipped with a thermally conductive strip in which the tubular meanders are pressed. So, it can ensure optimal heat conduction between the exchanger and PCM layer. Infrared thermography (IR) was performed to verify the temperature homogeneity, see Fig. 5. As can be seen, the temperature distribution is appropriate.

Fig. 6 shows the basic hydraulic scheme of the system. As can be seen, the hydraulic circuit is connected to the mobile heat exchanger. The connection also includes a circulation pump, distribution manifold, precise flow meter, and other sensors. The supply pipes to the cooling devices are routed behind the cover wall and are connected directly to the individual ceiling units. So, the system can be operated in active and passive form as well. In the standard passive mode, the technology uses the accumulation of heat or cold by PCM from the ambient. This mode is able to reduce temperature fluctuations and stabilize air temperature during the day and night. In passive mode, the system accumulates heat or cold without any external energy supply. In the active mode, it is able

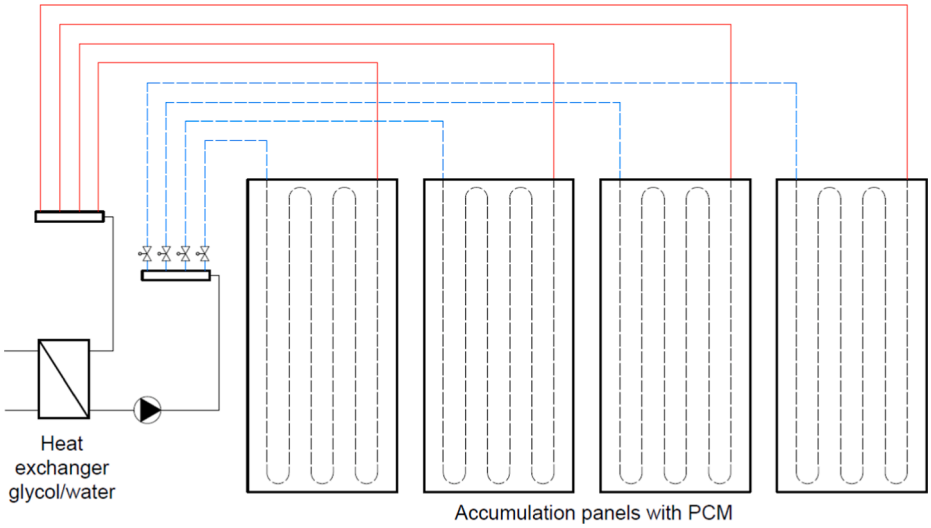

Fig. 6. Hydraulic connection of the cooling ceiling system.

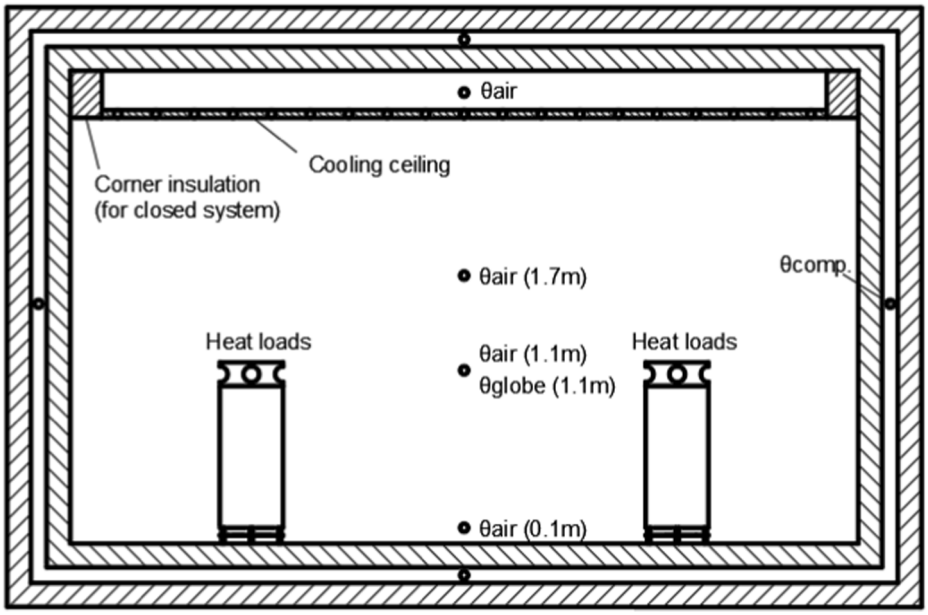

Fig. 7. Scheme of measuring space.

Fig. 8. Experimental measurement of PCM panels in a compensated chamber.

to influence the indoor temperature by the accumulated heat or cold obtained from any external sources, such as boiler, heat pump, chiller, or free cooling.

In the proposed ceiling system, the heat transfer medium is water. The water temperature is set according to the set-point and has to be kept above the dew point temperature. The cooling source requirement is a temperature of approx. 10 °C to 16 °C. This device's operation is energy efficient, and with sufficient cooling area, it is possible to ensure comfortable microclimatic conditions.

3.4. Test methodology for chilled ceilings - experiments

The test methodology is based on CSN EN 14240 and CSN EN 15116 [53,54]. The installation of the cooling ceiling panels and other elements is shown in Fig. 7. The ceiling units were installed in the space under the ceiling as an open system. For comparison, ceiling cooling measurements were performed with and without the PCM. Heat transfer to the ambient is given only by natural convection without forced convection.

The measurements are limited by the thermal technical properties of the measuring space (reconditioning chamber). For this reason, the necessary modifications were made to the Indoor part of CCC. Measurements inside the chamber are conditioned by airtightness and good thermal insulation properties of the structure. These conditions make it possible to set and keep required boundary conditions and minimize heat loss through the surrounding walls. The area should be in the range of 10 m^2 to 21 m^2 with a height of 2.7 m to 3 m.

First, all surfaces inside the measuring chamber were modified to ensure a high emissivity value. Furthermore, it was necessary to create a partition, which covered the reconditioning unit and the mobile heat exchanger station. For this purpose, a steel structure with PVC boards was realized. The modified reconditioning space with installed cooling ceilings and heat load simulators can be seen in Fig. 8.

During the test, it was necessary to ensure minimal heat loss through the surrounding walls. Therefore, the air temperatures in the surrounding compensation space and the adjacent space were kept the same as in the Indoor reconditioning space.

Electrically heated dummies do the heat load inside the chamber. The electrical input is adjustable with a maximum of 180 W per dummie. The maximum internal heat load can be up to 200 $W{\cdot}m^{-2}$. During the measurement, it was necessary to observe the required heat load values and maintain the ambient air temperature according to the normative requirements regarding the cooling capacity of the cooling ceiling.

All necessary parameters are recorded throughout the all experiments, such as air temperatures in the test chamber and surrounding spaces, humidity, surface temperatures of walls and the cooling ceiling, inlet and outlet temperatures of the coolant, mass flow rates, heat fluxes, and controlled heat load.

After the prototype realization and the measuring space preparation, it was possible to perform the following experiments: cooling capacity measurement, discontinuous cooling cycle, and heat absorption from the ambient. The methodology of each experiment is described in the following subsections.

3.4.1. Cooling capacity

One of the most important parameters of each active cooling ceiling system is its specific cooling capacity. The measurement is performed according to the normative requirements [53]. Measurement shall be carried out in steady-state conditions for at least three differences between air temperature and mean cooling water temperature of $\Delta T = T \pm 1$ K, where $T = \{6; 8; 10\}$K. The reference room temperature shall be between 22 °C and 27 °C. The cooling water inlet temperature shall be at least 2 K higher than the dew point temperature of the test room air. The standard also requires at least 60 min of steady-state conditions, during which the cooling capacity is measured [53].

The total cooling capacity of the cooling ceiling is given by the equation:

$$P = \dot{m} c_p (\theta_{w,out} - \theta_{w,in}), \quad (1)$$

where	P	total cooling capacity	(W),
	$\dot{m}$	mass flow rate	($kg{\cdot}s^{-1}$),
	c_p	specific heat capacity	($Jkg^{-1}K^{-1}$),
	$\theta_{w,out}$	outlet temperature	(°C),
	$\theta_{w,in}$	inlet temperature	(°C).

The specific cooling capacity can be determined by equations:

$$P_a = \frac{P}{A_a}, \quad (2)$$

where	P_a	specific cooling capacity	(Wm^{-2}),
	A_a	active cooling area	(m^2).

3.4.2. Discontinuous cooling cycle of cooling ceiling with PCM

The application of PCM inside cooling ceilings mainly increases its heat storage capacity. The subject of this experiment is to verify the behavior of the cooling ceiling system during shutdown and to determine how a discontinuous cooling cycle affects the thermal inertia of the cooling ceiling system with and without PCM.

The experiment consists of three parts: steady-state, cooling discontinuation, and active cooling. First, a steady-state conditions are reached: inside air temperature 26 °C, the temperature of all surrounding surfaces 26 °C, coolant flow rate 5 $l{\cdot}min^{-1}$ and inlet coolant temperature 10 °C. The heat load is set depending on the current cooling capacity. The steady-state conditions should last at least 90 min. Then

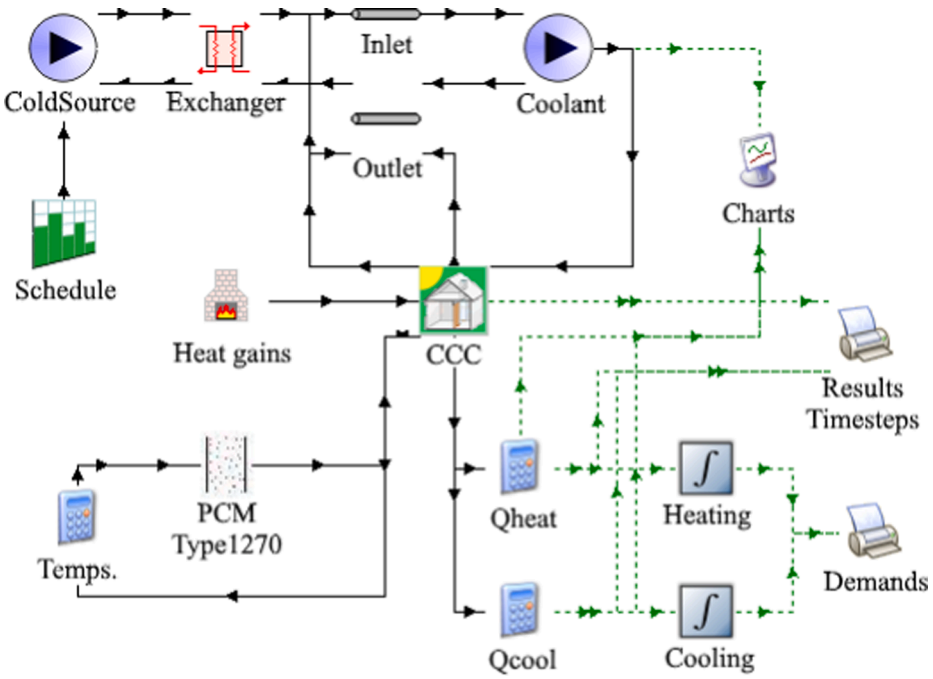

Fig. 9. Schema of TRNSYS calculation model - experiment.

the cooling source is shut down for 90 min. The circulating pump is switched off during this period, but the heat load is still switched on. These conditions cause the air temperature to increase, whereas a part of the heat load is absorbed into the PCM. Finally, the cooling source and circulation pump are switched on. This part should last until the initial conditions are reached.

3.4.3. *Heat load absorption*

This experiment is aimed to verify the behavior of the cooling ceiling system in conditions with external heat loads and cyclic regeneration of the PCM.

During the test, the heat is transferred through the cover partition to the test space. Behind the cover partition, the air temperature is kept in the range of 40 °C to 42 °C. The air temperatures in the other surrounding spaces are maintained at 24 °C throughout the measurement. The initial air temperature in the test space is 23 °C. The microclimatic conditions created in this way are simulations of the real conditions in the building, which is exposed to an external heat load through the walls.

The heat load causes the increase of air temperature and the charging of PCM. According to normative requirements, it is necessary to use active cooling when the air temperature is above 27 °C. So, the active cooling is switched on when the air temperature reaches this limit. It leads to PCM regeneration by dissipating the stored thermal energy by the coolant. When the cooling ceiling is cooled down, the active cooling is switched off. The PCM is then able to re-absorb the heat load inside the room and eliminate its overheating. After switching off the cooling, the heat load causes air temperature to increase up to the limit of 27 °C again, and the subsequent regeneration cycle is monitored.

The heat load is determined using the measurement of heat flux, air temperature, and partition surface temperature.

3.5. *Simulation models*

The presented research deals with PCM applications in HVAC systems, where it is possible to use these materials' passive and active properties for energy savings and thermal comfort improvement. In this part, the aim was to assess the effect of thermal energy accumulation on space cooling energy demand and thermal comfort. The TRNSYS and Ansys simulation SW was used to assess. The ANSYS software (SpaceClaim and Fluent) was used mainly to design the 3D model of the PCM-based cooling ceiling box and its transient thermal simulations. The TRNSYS was the most important for our purposes. This simulation software was used for the complex transient simulations. The simulation model of the proposed cooling ceiling panels with PCM had to be created and parametrized before the complex building energy simulations.

The simulation of the experiment was modeled in TRNSYS by Multi-Zone Building (Type56) with necessary components, such as PCM (Type1270), pumps (Type3), pipes (Type31), a heat exchanger (Type5), forcing functions (Type14h and Type14c), and others (plotters, equation, integrations, etc.), see Fig. 9.

Type 1270 is a simple PCM model designed to interact with Type 56 (building model). The phase change process has a constant temperature associated with a latent heat of fusion. The PCM has constant specific heat capacities in the solid and the liquid state. Type1270 has the task of calculating the PCM temperature at each time step as a function of the energies coming from the boundary layers (calculated by Type56). Then, a feedback loop at each time step is created. When the PCM material is in the transition phase, the temperature maintains constant, and the latent heat of fusion is compared with the energy coming from boundary layers. If the PCM layer can store this energy, then the absorbed or released energy is recorded, and a value of the liquid fraction is computed. If the storage capacity is exceeded, then the excess energy is conversed to sensible heat.

The Type56 representing the CCC was set as space without the influence of the external environment. The space was equipped with an active chilled ceiling with an additional PCM layer. The chilled ceiling parameters were set according to the tested cooling ceiling system. The settings of each other components were adjusted according to the real conditions of the experiment, such as air temperature, flow rates, heat exchanger and pipes parameters, internal heat load, and cooling operation schedule. This simulation model was validated according to real experiments performed in the CCC.

Concerning the possibility of comparing the results of simulations and measurements, the most important parameters are the coolant inlet and outlet temperatures, cooling ceiling surface temperature, and ambient temperature. The coolant temperature difference and flow rate determine the cooling power removed from the cooling ceiling.

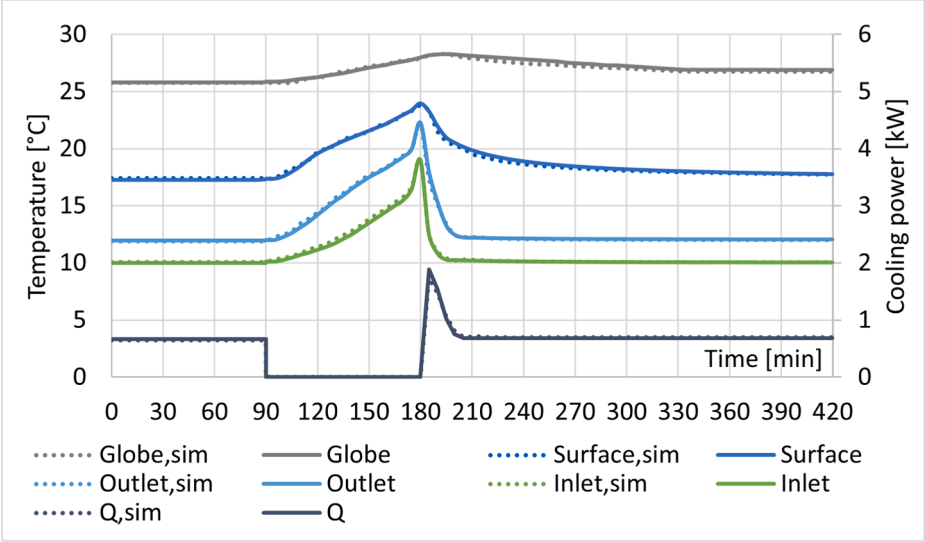

Fig. 10. Simulation validation.

Table 2
The indicators for the quality of the simulations.

Parameter	RMSE [± unit]	RRMSE [–]	R^2 [–]
Operative (globe) temperature	±0.178 °C	0.7	0.979
Ceiling surface temperature	±0.162 °C	0.9	0.992
Coolant inlet temperature	±0.128 °C	1.2	0.997
Coolant outlet temperature	±0.123 °C	0.9	0.997
Cooling power	±0.022 kW	4.0	0.995

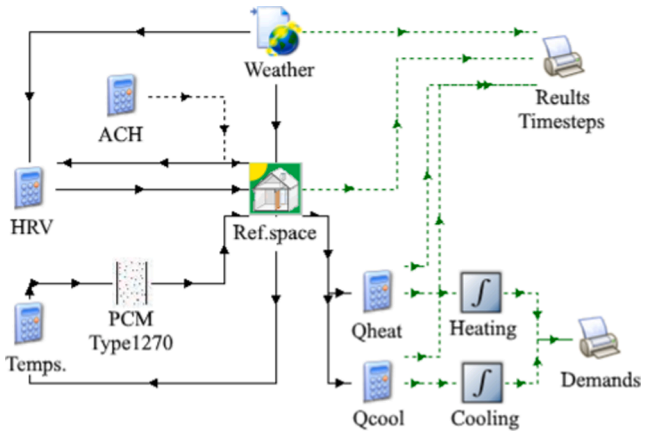

Fig. 11. Schema of TRNSYS calculation model - reference space.

For example, the obtained simulation results were compared with measurement of discontinuous cooling cycle of the cooling ceiling with PCM (Section 4.2), see Fig. 10. Concerning the possibility of comparison, the most important parameters were the coolant inlet and outlet temperatures, cooling ceiling surface temperature, and ambient temperature. The coolant temperature difference and flow rate determine the cooling power removed from the cooling ceiling.

The indicators for the quality of the simulations are the Root Mean Square Error (RMSE), the Relative Root Mean Square Error (RRMSE), and coefficient of determination R2. The RRMSE is calculated by dividing RMSE by the average value of the measured data. The more accurate simulation has lower RMSE and RRMSE. The results of the validation are depicted in Table 2.

According to the RMSE values, the simulated and measured data show a very good agreement. The validated PCM-based cooling ceiling model could be used in complex simulations with good accuracies.

The complex simulation model contains Multi-Zone Building (Type56), PCM layer module (Type1270), weather data reader (Type15), and other auxiliary modules (calculations, conversions, and numerical and graphical outputs), see Fig. 11. Weather profiles were obtained from our weather station (Zlin, Czechia, Central Europe, average values from 2017 to 2019) and transformed to the TMY2 format. The weather dataset includes values of location, dry bulb temperature, relative humidity, atmospheric pressure, solar radiation, wind direction, and wind speed.

The reference space model was characterized through TRNBuild, including building elements, occupancy schedules, air change rates, internal gains, and other aspects. Fig. 12 shows the schema of the reference room/space model.

The simulated space module was set to a reference model that has the following parameters:

- Dimensions: 5 × 4 × 2.7 m
- Exposure of the envelope from all sides.
- Envelope - Ytong (300 mm) with polystyrene insulation (100 mm).
- Ceiling/roof - roofing, insulation wool (200 mm), plasterboard.
- Floor - concrete with insulation (80 + 20 mm).
- Windows and doors oriented to the South, East, and West, 8 m^2.
- Exterior window shading - shading factor 0.5.
- Heat recovery ventilation (HRV) (efficiency 75%).
- Heat and cold source: air-to-water heat pump (HP) (3.1 COP, 2.5 EER).
- Air change rate (ACH) value is ranged between 0 h^{-1} and 2.5 h^{-1}.
- Active chilled ceiling/ active PCM-based chilled ceiling.
- The simulation time step was set at 60 s.

Occupancy schedules and internal gains were implemented as a daily profile. The total heat flow rate from occupants, appliances, and lighting was specified according to Annexe of CSN EN ISO 52016-1 [55], see Table 3.

4. Results and discussion

This chapter contains the results of various experiments performed according to the considered methodology described in Section 3.4 and

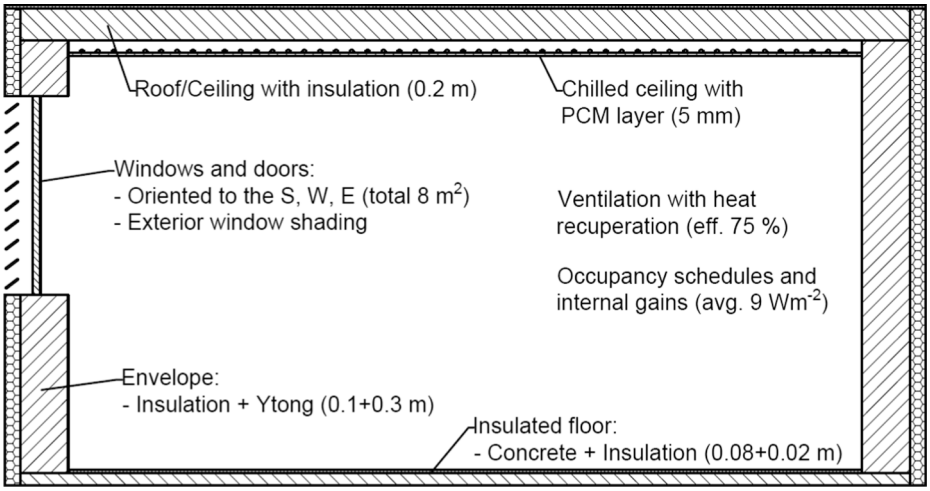

Fig. 12. Schema of reference room/space model.

Table 3
Total heat flow rate from occupants, appliances, and lighting (living room, residential building).

Time	Total heat flow [Wm^{-2}]
7:00–17:00	8.0
17:00–23:00	20.0
23:00–7:00	2.0
Average	9.0

the subsequent validation of the simulation data.

Three different experiments were performed: cooling capacity measurement, discontinuous cooling cycle, and heat absorption from the ambient.

4.1. Cooling capacity

This experiment was performed according to the procedure set out in Section 3.4.1. The cooling capacity was determined at four measurement points $\Delta T = \{6; 8; 10; 12\}$K and at coolant flow rate of 5 $l{\cdot}min^{-1}$. The air temperature inside the test space was kept between 26 °C and 27 °C during all measurements. The dew point value was around 10 °C during the tests. So, it was possible to perform measurements with a low coolant temperature.

Each measurement required time to stabilize the air temperature. The regulated heat load was set to ensure steady-state conditions considering the cooling capacity of the cooling ceilings. In the case of cooling ceilings with PCM, the time was twice as long as without PCM to ensure accuracy.

Fig. 13 shows the total and specific cooling capacity of the cooling ceilings with PCM. The total cooling capacity represents the capacity of all ceiling units with an active area of 4.67 m^2.

The cooling capacity results for the individual temperature differences are given in Table 4.

In the case of cooling ceiling units without PCM, the PCM layer was removed. The tube heat exchanger's thermally conductive strips were in direct contact with the surface of the cooling ceiling and thus caused a higher cooling capacity. The stabilization process was faster in this case

Table 4
Measurement of cooling capacity with PCM.

Measurement No.	1	2	3	4	
Mean temperature difference	12.21	10.24	8.26	6.26	K
Specific cooling capacity	108	90	73	55	Wm^{-2}
Total cooling capacity	503	422	341	260	W

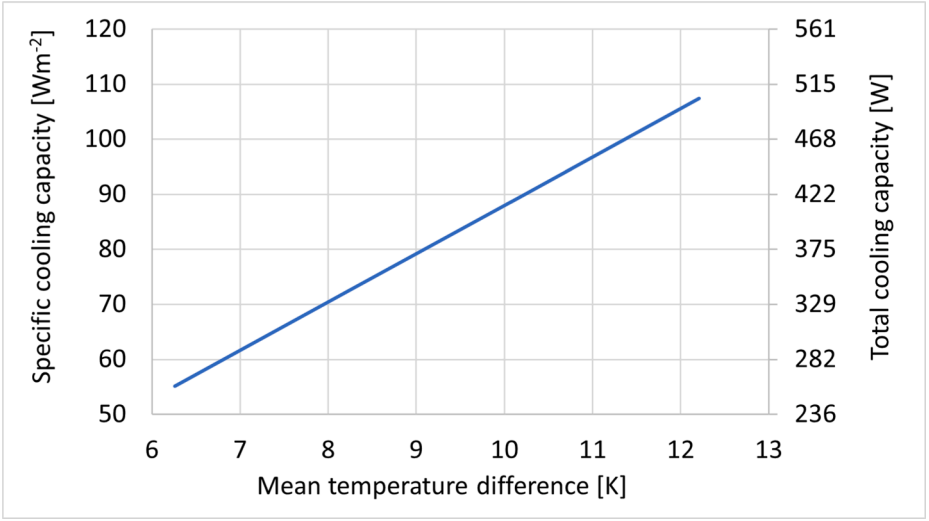

Fig. 13. Total and specific cooling capacity with PCM.

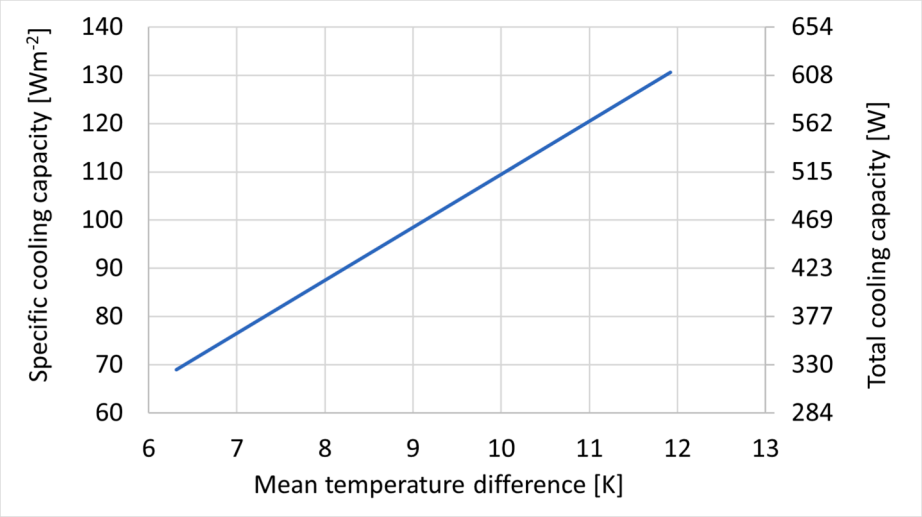

Fig. 14. Total and specific cooling capacity without PCM.

Table 5
Measurement of cooling capacity without PCM.

Measurement No.	1	2	3	4	
Mean temperature difference	11.92	10.16	7.97	6.31	K
Specific cooling capacity	131	111	87	69	Wm^{-2}
Total cooling capacity	611	521	410	325	W

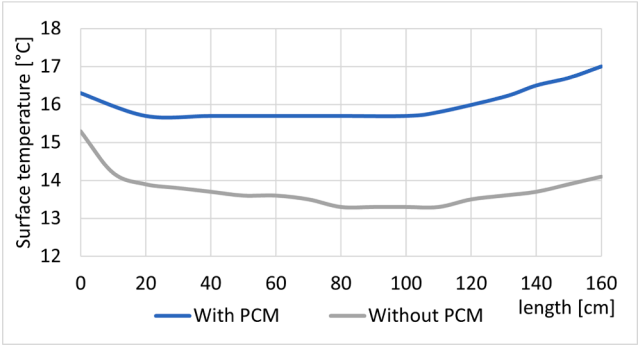

Fig. 15. Surface temperature distribution.

compared to the use of PCM. The stabilization of the process during the individual tests was significantly faster, and the system showed a faster response to temperature changes than was the case with the use of PCM. The measurement results are shown in Fig. 14 and Table 5.

The corrected specific cooling capacity of cooling ceiling units with PCM (nominal flow 5 l·min^{-1} and mean effective temperature difference 10 K) is around 87 Wm^{-2} and the capacity of units without PCM is around 109 Wm^{-2}.

The results of the cooling capacity measurement show a difference when the PCM is used. The cooling capacity with PCM was about 20% lower. It is caused by the relatively low thermal conductivity of the PCM. Although the PCM layer in the cooling ceiling is only 5 mm wide, the heat conduction is limited so that the surface temperature of the cooling unit is higher than in the case without PCM.

The surface temperature of each type of cooling unit was monitored by an IR camera during the test. Fig. 15 shows the distribution of average surface temperatures along the length of the cooling panel. As can be seen, the temperature distribution in the case with PCM is more homogenous, but the average surface temperature is higher by 2.3 °C.

4.2. Discontinuous cooling cycle

This experiment was performed according to the procedure set out in Section 3.4.2. The heat load was set at 586 W during the test to maintain the steady-state conditions. As shown in Fig. 16, the cooling source was turned off after 90 min of steady-state conditions. The cooling ceiling surface temperature increased significantly faster than the air temperature (globe temperature). The air temperature increased by 2.4 °C, from 25.8 °C to 28.2 °C, while the surface temperature increased by 6.9 °C, precisely from 16.6 °C to 23.5 °C. In the range between 21 °C and 22 °C, a change in the heating rate of the PCM is noticeable. It is due to the phase transition and the latent heat accumulation.

The measurement results show the system's behavior, which caused a very gradual increase in air temperature. It took about 4 h to reach almost the initial conditions after switching on the cooling. Thermal inertia is a time-consuming process due to the PCM application.

Measurement of discontinuous cooling was also performed for the cooling ceiling without the PCM layer. The measurement procedure and conditions were the same as in the previous case according to 3.4.2.

Fig. 17 shows the temperature profiles during the test of cooling ceilings without PCMs. The cooling capacity was higher, and the surface temperature was lower for the cooling ceiling units without PCM. So, the heat load had to be higher to ensure initial steady-state conditions; precisely, it was 679 W. Then, the cooling was turned off, and the heat load was set at 586 W to ensure the same conditions as measured with PCM. The electric heat load caused a significantly larger and faster rise in temperatures. The air temperature increased by 5.4 °C, from 26.2 °C to 31.6 °C, while in the test with PCM, it was only 2.4 °C. The surface temperature increased from 14.0 °C up to 30.8 °C. The heat load was set back to 679 W in the final part, and active cooling was switched on. The air temperature decreased significantly faster than in the previous case.

Fig. 18 shows a comparison of the results of measurements with and without PCM application. It can be seen a noticeable difference in the thermal inertia of a PCM-based cooling system. Switching off cooling caused a rapid rise in air temperature in the case of cooling ceilings without PCM. After switching on, the response of this system shows a fast response, and the air temperature drops faster than in the case with PCM. However, thanks to the lower temperature rise, the PCM-based system makes it possible to cool the air faster, even though the cooling units with PCM have a lower cooling capacity.

Experimental measurements confirmed the appropriate application of PCMs in the lower temperature range, where PCM has a very high value of specific heat capacity. The absorption of thermal energy confirmed this during the discontinuous cooling cycle.

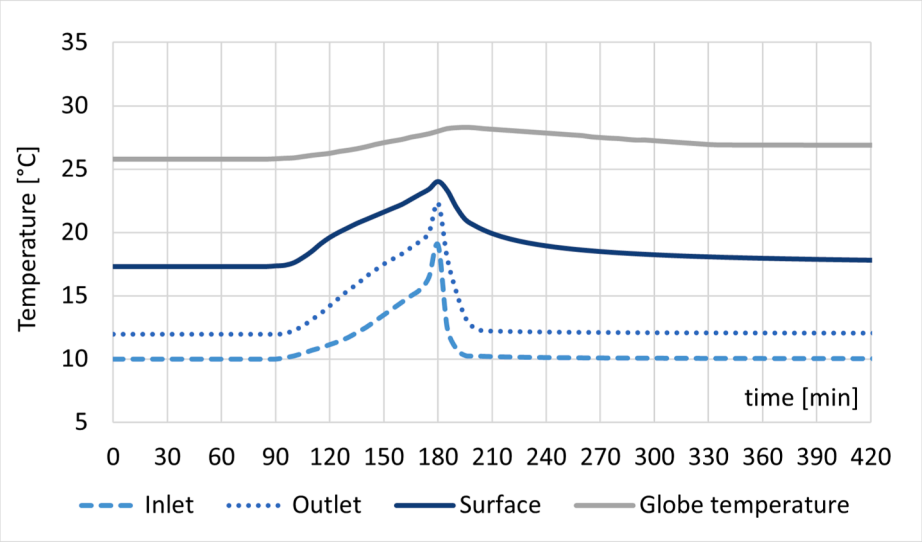

Fig. 16. Discontinuous cooling cycle with PCM.

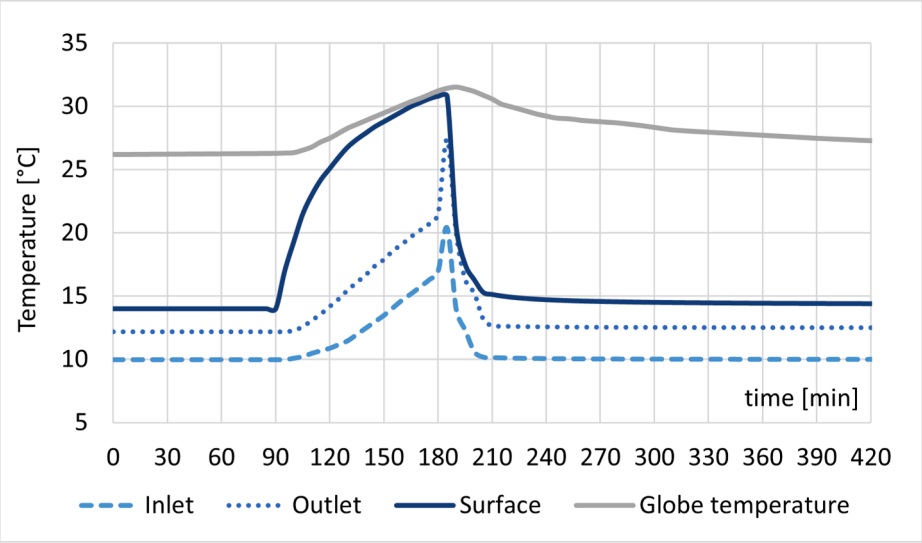

Fig. 17. Discontinuous cooling cycle without PCM.

4.3. Heat load absorption by PCM-based cooling ceilings

The heat load absorption experiment was evaluated by cyclic regeneration of the PCM according to the procedure set out in Section 3.4.3.

Fig. 19 shows the temperature profiles from the beginning of the measurement. The initial air temperature was 23 °C. The active cooling was switched on when the globe temperature reached 27 °C. The cooling operation time was 120 min (non-zero coolant flow rate), and the coolant temperature was 10 °C. After switching off the cooling, the air temperature increased very gradually. It then took around 90 min to reach the air temperature limit of 27 °C again. After that, the active cooling was switched on again. The second cooling cycle had similar results as the previous one. The phase transition is highlighted by the dashed line (21.5 °C) in the graph. It is noticeable the change in the heating rate of the PCM around this temperature. The total external heat load was around 350 W.

The dew point temperature was also monitored during the test. Throughout the measurement, the dew point temperature ranged from 11 °C to 13 °C, while the lowest surface temperature of the cooling ceiling was 17.7 °C.

The heat load absorption experiment was also performed to verify the discontinuous cooling by the PCM-based cooling ceilings. If the rooms are exposed to a large heat load, gradual overheating occurs during the day, which leads to needing to use air conditioning. Regeneration of the PCM allows reaching the temperature below the phase change temperature, i.e., removing the stored latent heat energy from the PCM. This temperature was reached after 30 min during the presented experiment (coolant temperature of 10 °C). The PCM application in the active cooling system has been proven to be an effective process for ensuring the regeneration of the heat storage medium.

The use of cooling ceilings with PCM for absorption of heat load represents an interesting way to increase the accumulation's efficiency, reduce the cooling source's operation time, and minimize operating costs. It is an economical and energy-effective cooling ceiling system, and the negative effects on health are also minimized. For example, there is no swirling dust and no unpleasant flow of cold air.

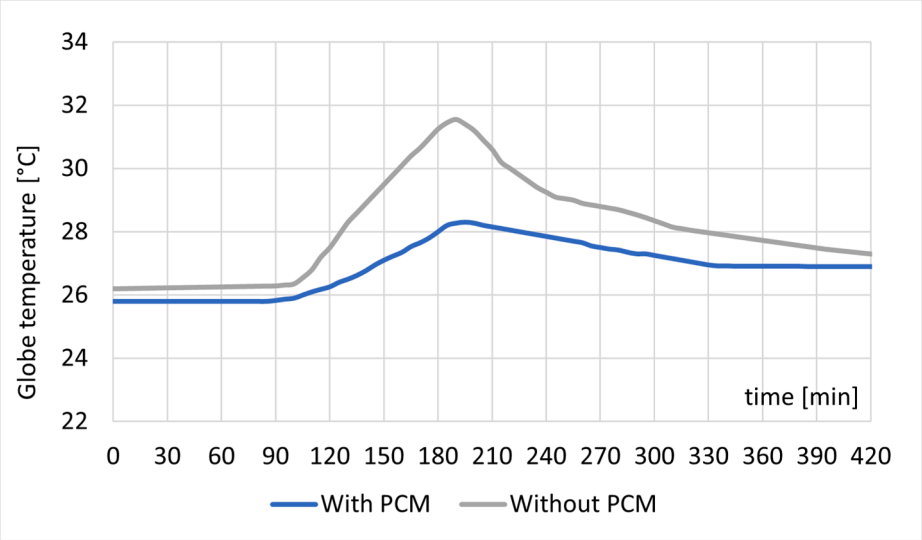

Fig. 18. Comparison of the results of measurements with and without PCM.

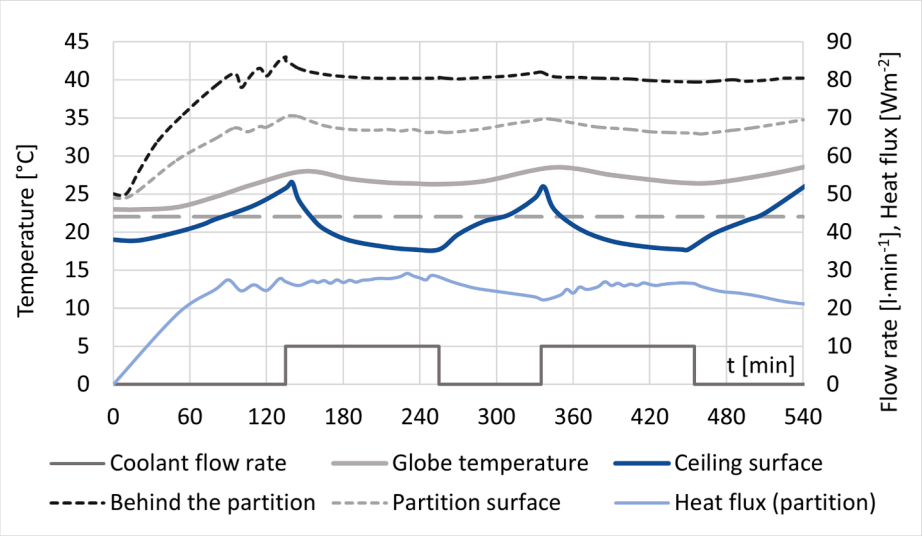

Fig. 19. Heat load absorption.

4.4. Accumulation and energy demand

The presented research deals with PCM application in cooling ceiling systems. This part aims to assess the effect of thermal energy accumulation on space cooling energy demand and thermal comfort. The validated simulation models according to practical applications and measurements in the LEE were used to assess, see 3.5.

Figs. 20 and 21 show the effect of using thermal energy storage. In the case of "without PCM", space is specified according to the parameters above. In the case of "with PCM", the inner part of the chilled ceiling is covered by 5 mm of PCM. As can be seen, the additional storage mass has a positive effect on stabilizing the operative temperature, and temperature peaks decreasing in general. The temperature peaks decreased by 1.5 °C to 3.2 °C (for ventilation intensity 2.0 h^{-1}), see Fig. 20.

Fig. 21 shows the impact of accumulation (indexes PCM) and different ACH on operative temperature. The chart represents average values of the maximum, mean, and minimum operative temperatures during the seven days, as in Fig. 20.

Besides stabilizing the operative temperature, the additional storage mass has a positive effect on reducing the energy demand for cooling and heating. Within the performed simulations, the effect of the application of additional accumulation mass in combination with different ACH was observed.

The main area of interest was space cooling in the summer months - from May to September. In this period, the need for mechanical cooling was identified. The cooling requirements were limited by the maximum permissible operative temperature established at 26 °C. Table 6 shows the final energy consumption for space cooling and possible energy savings concerning different values of ACH.

For the overall energy and economic evaluation, it is necessary to know the total annual energy consumption, including cooling and space heating. As already mentioned, the permissible operative temperature was set at a maximum of 26 °C in summer and a minimum of 20 °C in winter. Table 7 shows the annual total final energy consumption and possible savings.

The results show that the additional or the lack of accumulation mass significantly affects HVAC systems' energy consumption. In general, the final energy consumption is increasing for cooling and decreasing for heating when ACH is lowering. When the ACH is low, the energy demand for cooling increases during the summer because of the

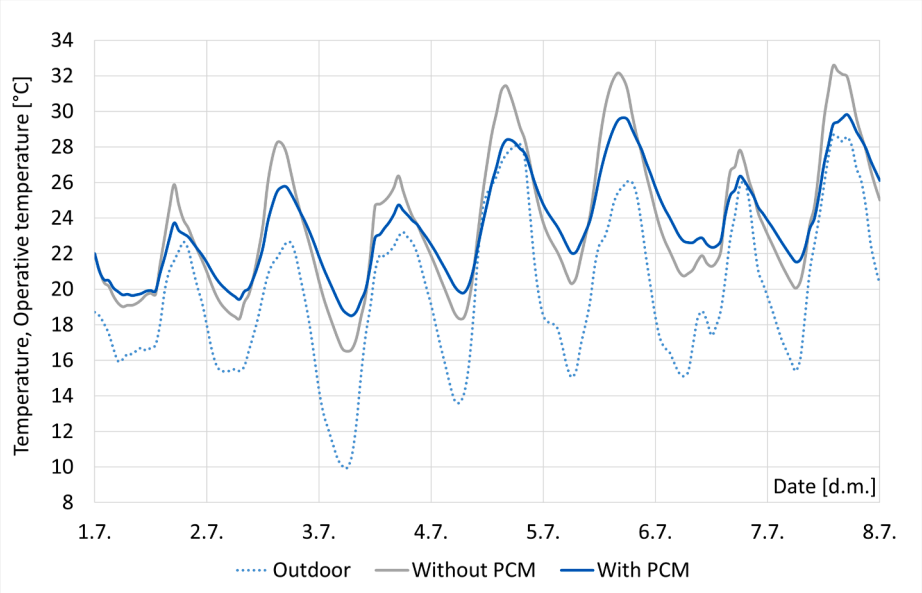

Fig. 20. Outdoor and indoor operative temperatures.

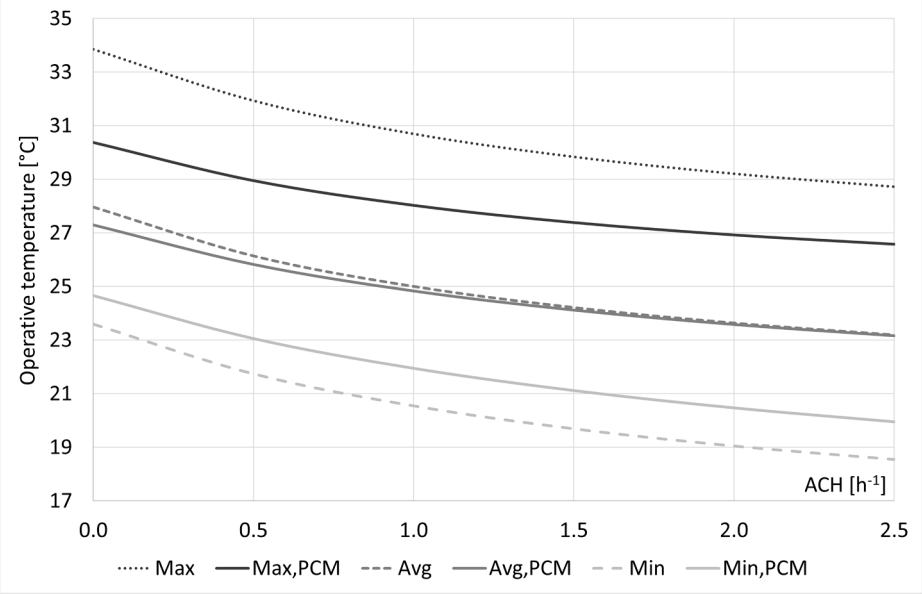

Fig. 21. Impact of different ACH on operative temperature.

Table 6
Final energy consumption for space cooling.

Air Change Rate [1·h^{-1}]	Without PCM [kWh]	With PCM [kWh]	Energy savings [kWh]	Energy savings [%]
0	390	348	45	10.8
0.5	334	286	48	14.4
1.0	299	245	54	18.1
1.5	276	216	60	21.8
2.0	258	194	64	24.9
2.5	246	178	68	27.5

Table 7
Annual total final energy consumption for space cooling and heating.

Air Change Rate [1·h^{-1}]	Without PCM [kWh]	With PCM [kWh]	Energy savings [kWh]	Energy savings [%]
0	1017	912	105	10.3
0.5	1070	950	121	11.3
1.0	1177	1041	136	11.5
1.5	1259	1109	150	11.9
2.0	1318	1157	161	12.2
2.5	1379	1211	168	12.2

overheating, while the heat losses by ventilation decrease during the winter. The PCM integration positively affects final energy consumption in all cases, and it is more effective as ACH increases.

4.5. *Financial performance valuation*

Finally, the proposed PCM-based cooling ceiling system is economically evaluated to define the Net Present Value (NPV), the Internal Rate

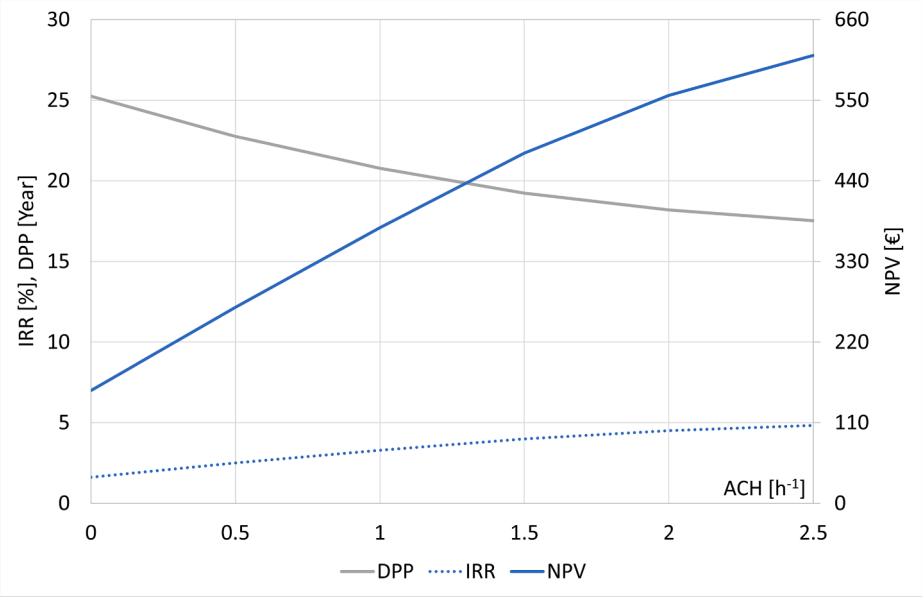

Fig. 22. Impact of different ACH on operative temperature.

of Return (IRR), and the Discounted Payback Period (DPP) of the investment. It is worth mentioning that its lifespan is defined for every single building component, referring to values given by Appendix A of EN 15459 [56]. The lifespan of the cooling ceilings is 30 years [56], although the lifespan of the PCM can be higher [57–59].

It is necessary to define the general financial data:

- Escalation of energy prices (Inflation rate): 2.8% [60]
- Discount rate: 0.25% [61]
- Lifespan: 30 years
- Price of electricity in Czechia (excl. VAT): €0.163/kWh [62]
- The cost of the PCM was estimated at €600

Fig. 22 shows the results of the financial performance evaluation of the proposed PCM-based cooling ceiling. As can be seen, the ACH is a very significant parameter.

In the case of 0 ACH, the discounted payback period of the investment is 25.3 years, the economic benefit at the end of the lifespan, expressed as NPV, is just €154, and the IRR is only 1.6%. If the ACH value is set to 2.5 h^{-1}, the DPP decreases at 17.5 years, the NPV increases at €611, and the IRR is 4.8%.

It should be mentioned that financial performance is highly dependent on the price of energy, inflation rate, and discount rate. These parameters are significantly different for each country. From the perspective of global environmental aims, it is important that reducing energy consumption is reached.

5. Conclusion

The presented article was focused on PCMs and showed a possible application of the PCM-based cooling ceiling system. The presented study analyzed the impact of PCM integration on cooling performance, thermal comfort, and cooling energy savings for the specific climate of Czechia. In the study, the PCM-based cooling ceiling's technical solution was performed, and the prototype was realized with performed simulations and experiments. The financial performance analysis was also performed.

Practical experiments of the proposed solution with and without PCM were performed. The results show a noticeable difference in the thermal inertia and cooling capacity of a PCM-based cooling system. The cooling capacity is about 20% lower, which is caused by the relatively low thermal conductivity of the PCM. Thus, the response of the basic solution is faster. However, the PCM-based solution shows lower air temperature fluctuations and requires less cooling power in the final consequence.

The tests and experiments performed have had generally positive results. The PCM-based cooling ceiling system can significantly improve thermal comfort (reduction air temperature fluctuations and peaks by up to 3.2 °C) and bring up to 27.5% energy savings in space cooling.

The economic performance evaluation was performed where the DPP was calculated at 17.5 years, the NPV at €611, and the IRR at 4.8%, in the case of 2.5 ACH.

The proposed solution represents the modern possibility of combining passive and active systems to increase thermal comfort and energy savings. The significant benefit is the finding that the proposed solution is practically feasible.

Declaration of Competing Interest

The authors declare that they have no known competing financial interests or personal relationships that could have appeared to influence the work reported in this paper.

Acknowledgments

This work was supported by the European Regional Development Fund under the project CEBIA-Tech Instrumentation No. CZ.1.05/2.1.00/19.0376 and by the Ministry of Education, Youth and Sports of the Czech Republic within the National Sustainability Programme project No. LO1303 (MSMT-7778/2014) and also by the project INTERREG V-A SK-CZ/2019/11 No. NFP304010Y280.

References

[1] 2019 Global Status Report for Buildings and Construction: Towards a Zero-emissions, Efficient and Resilient Buildings and Construction Sector, Global Alliance for Buildings and Construction, International Energy Agency and the United Nations Environment Programme, 2019.
[2] Directive 2010/31/eu of the european parliament and of the council of 19 May 2010 on the energy performance of buildings, 2010.
[3] Directive (eu) 2018/844 of the european parliament and of the council of 30 May 2018 amending directive 2010/31/eu on the energy performance of buildings and directive 2012/27/eu on energy efficiency, 2018.

[4] K.J. Lomas, S.M. Porritt, Overheating in buildings: lessons from research, Build. Res. Inform. 45 (1–2) (2017) 1–18, https://doi.org/10.1080/09613218.2017.1256136.

[5] Energy performance of buildings - energy needs for heating and cooling, internal temperatures and sensible and latent heat loads - part 1: Calculation procedures, Standards, Office for Standards, Metrology and Testing, Praha, 2019.

[6] Thermal protection of buildings - part 2: Requirements, Standards, Office for Standards, Metrology and Testing, Praha (2011).

[7] U. Knaack, E. Koenders, Building Physics of the Envelope, Birkhäuser, Berlin, Basel, 2018.

[8] S. Ali, S. Deshmukh, An overview: Applications of thermal energy storage using phase change materials, Mater. Today: Proc. 26 (2020) 1231–1237, https://doi.org/10.1016/j.matpr.2020.02.247, 10th International Conference of Materials Processing and Characterization.

[9] D.N. Nkwetta, F. Haghighat, Thermal energy storage with phase change material—a state-of-the art review, Sustain. Cities Soc. 10 (2014) 87–100, https://doi.org/10.1016/j.scs.2013.05.007.

[10] S. Ali, S. Deshmukh, An overview: Applications of thermal energy storage using phase change materials, Materials Today: Proc. https://doi.org/10.1016/j.matpr.2020.02.247.

[12] L. Cabeza, A. Castell, C. Barreneche, A. de Gracia, A. Fernández, Materials used as pcm in thermal energy storage in buildings: A review, Renew. Sustain. Energy Rev. 15 (3) (2011) 1675–1695, https://doi.org/10.1016/j.rser.2010.11.018. URL https://www.sciencedirect.com/science/article/pii/S1364032110003874.

[13] M. Frigione, M. Lettieri, A. Sarcinella, Phase change materials for energy efficiency in buildings and their use in mortars, Materials 12. https://doi.org/10.3390/ma12081260.

[14] J. Heier, C. Bales, V. Martin, Combining thermal energy storage with buildings - a review, Renew. Sustain. Energy Rev. 42 (2015) 1305–1325, https://doi.org/10.1016/j.rser.2014.11.031. URL https://www.sciencedirect.com/science/article/pii/S1364032114009629.

[15] J. Belmonte, P. Eguía, A. Molina, J. Almendros-Ibáñez, Thermal simulation and system optimization of a chilled ceiling coupled with a floor containing a phase change material (pcm), Sustain. Cities Soc. 14 (2015) 154–170, https://doi.org/10.1016/j.scs.2014.09.004. URL https://www.sciencedirect.com/science/article/pii/S2210670714001024.

[16] K.O. Lee, M.A. Medina, X. Sun, X. Jin, Thermal performance of phase change materials (pcm)-enhanced cellulose insulation in passive solar residential building walls, Sol. Energy 163 (2018) 113–121, https://doi.org/10.1016/j.solener.2018.01.086. URL https://www.sciencedirect.com/science/article/pii/S0038092X18301075.

[17] C. Yao, X. Kong, Y. Li, Y. Du, C. Qi, Numerical and experimental research of cold storage for a novel expanded perlite-based shape-stabilized phase change material wallboard used in building, Energy Convers. Manage. 155 (2018) 20–31, https://doi.org/10.1016/j.enconman.2017.10.052. URL https://www.sciencedirect.com/science/article/pii/S0196890417309858.

[18] M.T. Plytaria, E. Bellos, C. Tzivanidis, K.A. Antonopoulos, Numerical simulation of a solar cooling system with and without phase change materials in radiant walls of a building, Energy Convers. Manage. 188 (2019) 40–53, https://doi.org/10.1016/j.enconman.2019.03.042. URL https://www.sciencedirect.com/science/article/pii/S0196890419303371.

[19] Q. Wang, R. Wu, Y. Wu, C. Zhao, Parametric analysis of using pcm walls for heating loads reduction, Energy Build. 172 (2018) 328–336, https://doi.org/10.1016/j.enbuild.2018.05.012. URL https://www.sciencedirect.com/science/article/pii/S0378778818302202.

[20] Q. Li, L. Ma, D. Li, M. Arici, Çagatay Yildiz, Z. Wang, Y. Liu, Thermoeconomic analysis of a wall incorporating phase change material in a rural residence located in northeast china, Sustain. Energy Technol. Assessm. 44 (2021) 101091, https://doi.org/10.1016/j.seta.2021.101091. URL https://www.sciencedirect.com/science/article/pii/S2213138821001016.

[21] G. Pavlov, Building thermal energy storage., Ph.D. thesis (2014).

[22] C. Yang, G. Susman, M. Dowson, Energyplus model of novel pcm cooling system validated with installed system data, Proc. SimBuild 6 (1).

[23] S. Rucevskis, P. Akishin, A. Korjakins, Performance evaluation of an active pcm thermal energy storage system for space cooling in residential buildings, Environ. Climate Technol. 23 (2) (2019) 74–89, https://doi.org/10.2478/rtuect-2019-0056.

[24] H. Weinläder, F. Klinker, M. Yasin, Pcm cooling ceilings in the energy efficiency center–passive cooling potential of two different system designs, Energy Build. 119 (2016) 93–100, https://doi.org/10.1016/j.enbuild.2016.03.031. URL https://www.sciencedirect.com/science/article/pii/S0378778816301682.

[25] H. Weinläder, F. Klinker, M. Yasin, Pcm cooling ceilings in the energy efficiency center – regeneration behaviour of two different system designs, Energy Build. 156 (2017) 70–77, https://doi.org/10.1016/j.enbuild.2017.09.010. URL https://www.sciencedirect.com/science/article/pii/S0378778817321540.

[26] Dragos-Ioan Bogatu, Eleftherios Bourdakis, Ongun Berk Kazanci, Bjarne W. Olesen, Experimental comparison of radiant ceiling panels and ceiling panels containing phase change material (pcm), E3S Web Conf. 111 (2019) 01072, https://doi.org/10.1051/e3sconf/201911101072.

[27] D.-I. Bogatu, O.B. Kazanci, B.W. Olesen, An experimental study of the active cooling performance of a novel radiant ceiling panel containing phase change material (pcm), Energy Build. 243 (2021) 110981, https://doi.org/10.1016/j.enbuild.2021.110981. URL https://www.sciencedirect.com/science/article/pii/S0378778821002656.

[28] D. Li, Y. Wu, G. Zhang, M. Arici, C. Liu, F. Wang, Influence of glazed roof containing phase change material on indoor thermal environment and energy consumption, Appl. Energy 222 (2018) 343–350, https://doi.org/10.1016/j.apenergy.2018.04.015. URL https://www.sciencedirect.com/science/article/pii/S0306261918305592.

[29] I. Vigna, L. Bianco, F. Goia, V. Serra, Phase change materials in transparent building envelopes: A strengths, weakness, opportunities and threats (swot) analysis, Energies 11(1). https://doi.org/10.3390/en11010111. https://www.mdpi.com/1996-1073/11/1/111.

[30] S. Li, G. Sun, K. Zou, X. Zhang, Experimental research on the dynamic thermal performance of a novel triple-pane building window filled with pcm, Sustain. Cities Soc. 27 (2016) 15–22, https://doi.org/10.1016/j.scs.2016.08.014. URL https://www.sciencedirect.com/science/article/pii/S2210670716302244.

[31] T. Silva, R. Vicente, F. Rodrigues, Literature review on the use of phase change materials in glazing and shading solutions, Renew. Sustain. Energy Rev. 53 (2016) 515–535, https://doi.org/10.1016/j.rser.2015.07.201. URL https://www.sciencedirect.com/science/article/pii/S1364032115009053.

[32] M. Song, F. Niu, N. Mao, Y. Hu, S. Deng, Review on building energy performance improvement using phase change materials, Energy Build. 158 (2018) 776–793, https://doi.org/10.1016/j.enbuild.2017.10.066. URL https://www.sciencedirect.com/science/article/pii/S037877881732916X.

[33] B. Jelle, S. Kalnæs, Chapter 3 - phase change materials for application in energy-efficient buildings, in: F. Pacheco-Torgal, C.-G. Granqvist, B.P. Jelle, G.P. Vanoli, N. Bianco, J. Kurnitski (Eds.), Cost-Effective Energy Efficient Building Retrofitting, Woodhead Publishing, 2017, pp. 57–118, https://doi.org/10.1016/B978-0-08-101128-7.00003-4.

[34] Quesada Allerhand, Berk Kazanci José, Olesen Ongun, W. Bjarne, Energy and thermal comfort performance evaluation of pcm ceiling panels for cooling a renovated office room, E3S Web Conf. 111 (2019) 03020, https://doi.org/10.1051/e3sconf/201911103020.

[35] A. Madad, T. Mouhib, A. Mouhsen, Phase change materials for building applications: A thorough review and new perspectives, Buildings 8(5). https://doi.org/10.3390/buildings8050063. https://www.mdpi.com/2075-5309/8/5/63.

[36] H. Weinläder, W. Körner, B. Strieder, A ventilated cooling ceiling with integrated latent heat storage—monitoring results, Energy Build. 82 (2014) 65–72, https://doi.org/10.1016/j.enbuild.2014.07.013. URL https://www.sciencedirect.com/science/article/pii/S0378778814005507.

[37] M. Alizadeh, S. Sadrameli, Indoor thermal comfort assessment using pcm based storage system integrated with ceiling fan ventilation: Experimental design and response surface approach, Energy Build. 188–189 (2019) 297–313, https://doi.org/10.1016/j.enbuild.2019.02.020. URL https://www.sciencedirect.com/science/article/pii/S0378778818332717.

[38] Y. Zhou, C.W. Yu, G. Zhang, Study on heat-transfer mechanism of wallboards containing active phase change material and parameter optimization with ventilation, Appl. Therm. Eng. 144 (2018) 1091–1108, https://doi.org/10.1016/j.applthermaleng.2018.04.083. URL https://www.sciencedirect.com/science/article/pii/S135943111830440X.

[39] S. Liu, M. Iten, A. Shukla, Numerical study on the performance of an air—multiple pcms unit for free cooling and ventilation, Energy Build. 151 (2017) 520–533, https://doi.org/10.1016/j.enbuild.2017.07.005. URL https://www.sciencedirect.com/science/article/pii/S0378778816320138.

[40] R. Barzin, J.J. Chen, B.R. Young, M.M. Farid, Application of pcm energy storage in combination with night ventilation for space cooling, Appl. Energy 158 (2015) 412–421, https://doi.org/10.1016/j.apenergy.2015.08.088. URL https://www.sciencedirect.com/science/article/pii/S0306261915010247.

[41] E. Bourdakis, T.Q. Péan, L. Gennari, B.W. Olesen, Daytime space cooling with phase change material ceiling panels discharged using rooftop photovoltaic/thermal panels and night-time ventilation, Sci. Technol. Built Environ. 22 (7) (2016) 902–910, https://doi.org/10.1080/23744731.2016.1181511.

[42] M. Koschenz, B. Lehmann, Development of a thermally activated ceiling panel with pcm for application in lightweight and retrofitted buildings, Energy Build. 36 (6) (2004) 567–578, https://doi.org/10.1016/j.enbuild.2004.01.029. URL https://www.sciencedirect.com/science/article/pii/S0378778804000702.

[43] T. Yan, Z. Sun, J. Gao, X. Xu, J. Yu, W. Gang, Simulation study of a pipe-encapsulated pcm wall system with self-activated heat removal by nocturnal sky radiation, Renew. Energy 146 (2020) 1451–1464, https://doi.org/10.1016/j.renene.2019.07.060. URL https://www.sciencedirect.com/science/article/pii/S0960148119310808.

[44] Y. Zhou, S. Zheng, G. Zhang, Study on the energy performance enhancement of a new pcms integrated hybrid system with the active cooling and hybrid ventilations, Energy 179 (2019) 111–128, https://doi.org/10.1016/j.energy.2019.04.173. URL https://www.sciencedirect.com/science/article/pii/S0360544219308060.

[45] J. Skovajsa, M. Zalesak, The use of the photovoltaic system in combination with a thermal energy storage for heating and thermoelectric cooling, Appl. Sci. 8. https://doi.org/10.3390/app8101750.

[46] J. Skovajsa, M. Kolacek, M. Zalesak, Phase change material based accumulation panels in combination with renewable energy sources and thermoelectric cooling, Energies 10 (2017) 152, https://doi.org/10.3390/en10020152.

[47] L.F. Nielsen, E. Bourdakis, O.B. Kazanci, B.W. Olesen, The influence of a radiant panel system with integrated phase change material on energy use and thermal indoor environment, in: Proceedings of the ASHRAE Winter Conference, 2018.

[48] A. Gallardo, U. Berardi, Analysis of the energy and thermal performance of a radiant cooling panel system with integrated phase change materials in very hot and humid conditions 609 (2019) 052025. https://doi.org/10.1088/1757-899x/609/5/052025.

[49] C. Stefansen, H. Farhan, E. Bourdakis, O.B. Kazanci, B.W. Olesen, Simulation study of performance of active ceilings with phase change material in office buildings under extreme climate conditions, in: ASHRAE 2018 Winter Conference, American Society of Heating, Refrigerating and Air-Conditioning Engineers, 2018.

[50] J. Gilbert, U. Koster, PCM Guidebook, DuPont Energain.
[51] F. Kuznik, J. Virgone, Experimental investigation of wallboard containing phase change material: Data for validation of numerical modeling, Energy Build. 41 (5) (2009) 561–570, https://doi.org/10.1016/j.enbuild.2008.11.022. URL https://www.sciencedirect.com/science/article/pii/S0378778808002673.
[52] The centre for security, information and advanced technologies (cebia – tech). https://fai.utb.cz/cebia-tech/.
[53] Ventilation for buildings - chilled ceilings - testing and rating, Standards, Office for Standards, Metrology and Testing, Praha (2004).
[54] Ventilation in buildings - chilled beams - testing and rating of active chilled beams, Standards, Office for Standards, Metrology and Testing, Praha (2008).
[55] Energy performance of buildings - energy needs for heating and cooling, internal temperatures and sensible and latent heat loads - part 1: Calculation procedures, Standards, Office for Standards, Metrology and Testing, Praha (2019).
[56] Energy performance of buildings - economic evaluation procedure for energy systems in buildings - part 1: Calculation procedures, module m1-14, Standards, Office for Standards, Metrology and Testing, Praha (2018).
[57] M. Mehrali, S.T. Latibari, M. Mehrali, H.S.C. Metselaar, M. Silakhori, Shape-stabilized phase change materials with high thermal conductivity based on paraffin/graphene oxide composite, Energy Convers. Manage. 67 (2013) 275–282, https://doi.org/10.1016/j.enconman.2012.11.023. URL https://www.sciencedirect.com/science/article/pii/S019689041200461X.
[58] M. Silakhori, M.S. Naghavi, H.S.C. Metselaar, T.M.I. Mahlia, H. Fauzi, M. Mehrali, Accelerated thermal cycling test of microencapsulated paraffin wax/polyaniline made by simple preparation method for solar thermal energy storage, Materials 6 (5) (2013) 1608–1620, https://doi.org/10.3390/ma6051608. URL https://www.mdpi.com/1996-1944/6/5/1608.
[59] Quality association pcm - pcm - phase change material. https://www.pcm-ral.org/pcm/en/quality-association-pcm/.
[60] Inflation - types, definition, tables — czso. https://www.czso.cz/csu/czso/inflation_rate.
[61] Discount rate (official cnb's interest rates (monthly average)) - czech republic statistics. https://eng.kurzy.cz/cnb/ekonomika/official-cnb-s-interest-rates-monthly-average/discount-rate/.
[62] Electricity price statistics. https://ec.europa.eu/eurostat/statistics-explained/index.php?title=Electricity_price_statistics.